Preparation of chitosan-based composite films with GG/QSM addition and investigation of their properties

Sevim Gürdaş Mazlum[1,2]*, Aslı Eda Erdoğan[2]

[1]Department of Chemical Engineering, Faculty of Engineering, Cumhuriyet University, Sivas, Turkey; [2]Department of Food Engineering, Faculty of Engineering, Cumhuriyet University, Sivas, Turkey

***Corresponding Author:** Sevim Gürdaş Mazlum, Department of Chemical Engineering, Faculty of Engineering, Cumhuriyet University, Turkey. Email: sgurdas@cumhuriyet.edu.tr

Academic Editor: Slim Smaoui, PhD, Laboratory of Microbial, Enzymatic Biotechnology and Biomolecules (LBMEB), Center of Biotechnology of Sfax, University of Sfax, Sfax, Tunisia

Received: 12 August 2025; Accepted: 24 November 2025; Published: 16 February 2026

ORIGINAL ARTICLE

Abstract

This study aims to produce chitosan (CH)-based composite films using CH, guar gum (GG), and quince seed mucilage (QSM) and to investigate the physicochemical, barrier, optical, mechanical, thermal, and microstructural properties of these films. CH-based composite films were fabricated by including three concentrations of GG and QSM (20–40%, v/v). Scanning electron microscopic analysis revealed that all composite films exhibited smooth and homogeneous surface morphologies, indicating good compatibility among the components. Fourier-transform infrared spectroscopy confirmed the formation of hydrogen bond interactions between constituent polymers. Differential scanning calorimetry demonstrated enhanced thermal stability in composite films relative to CH film. Optical property measurements indicated higher opacity values for all composite films compared to the CH film. Compared to the CH control film, the CH-GG-QSM1 composite film exhibits the lowest water solubility (WS) and water vapor permeability (WVP) values, while the CH-GG-QSM3 film exhibits the lowest moisture content (MC). Tensile strength (TS) of the CH-GG-QSM2 film increased by 14.58%, from 11.45 MPa to 13.12 MPa, while its elongation at break decreased by 3.28%, from 14.70% to 11.42%. At the same time, while the MC, WS and WVP values of the CH-GG-QSM2 composite film decreased compared to the CH film, it was determined that this composite film exhibited the best physicochemical properties. Strong linear correlations between physicochemical properties of composite films are determined using Pearson's correlation analysis. These findings indicate that the produced CH-GG-QSM composite films possess enhanced WVP, thermal stability, and optical properties. Consequently, they can demonstrate significant potential for application as edible packaging materials, particularly for preserving fruits, vegetables, and food products.

Keywords: chitosan; guar gum; quince seed mucilage; composite film; edible film

Introduction

Food packaging serves critical functions in preserving product quality and safety while ensuring integrity during transportation, storage, and distribution. Conventional materials, such as glass, metal, paper, and petroleum-derived plastics, dominate the industry. Among these, synthetic plastic films are particularly prevalent because of their low cost, flexibility, durability, transparency, and processability (Baghi *et al.*, 2022). However, the

proliferation of non-biodegradable, single-use plastic packaging generates persistent environmental pollution. Post-consumer plastic waste releases microplastics that contaminate marine, terrestrial, and food systems, posing significant ecological and human health risks (Baghi *et al.,* 2022; Maurizzi *et al.,* 2021). Heightened societal awareness of these impacts has accelerated the search for sustainable alternatives to petroleum-based packaging (Maurizzi *et al.,* 2021).

Edible films and coatings represent a promising approach for reducing reliance on conventional plastics. These materials, typically derived from edible biopolymers, such as polysaccharides, proteins, or lipids, can be consumed with packaged product, or degrade harmlessly (Maurizzi *et al.,* 2021; Narasagoudr *et al.,* 2023). While not a complete replacement for traditional packaging, edible films significantly diminish plastic usage and long-term environmental burden. Within biopolymer research, polysaccharides are extensively investigated due to their renewable sourcing, biodegradability, film-forming capacity, abundance, and low cost (Bhat *et al.,* 2022; Cazón *et al.,* 2017). Starch, cellulose, chitosan (CH), pectin, alginate, guar gum (GG), and plant mucilages are prominent examples. Composite films combining multiple biopolymers often exhibit superior thermal stability, mechanical strength, and barrier properties, compared to single-component films (Hiremani *et al.,* 2022; Priyadarshi and Rhim, 2020). Accordingly, this study utilizes CH, GG, and quince seed mucilage (QSM) to develop novel edible composite films.

One of the most important characteristics of a food packaging material is its biodegradability. When food packaging material reaches the end of its useful life, it is expected to return to nature, rather than accumulate as solid waste (Priyadarshi and Rhim, 2020). The biodegradability of biopolymers, such as CH, GG, and QSM, depends on enzymatic and hydrolytic degradation. Hydrolytic enzymes that break down these polymers are widely found in nature (Priyadarshi and Rhim, 2020; Sharma *et al.,* 2018). Lysozyme, found in bodily fluids, can easily digest these polymers, enabling them to be consumed along with food. Studies on biological degradability are generally conducted using burial and composting methods. In the burial method, samples are buried in soil and exposed to ambient temperatures. The biodegradability of examined samples is assessed by weight loss. The soil-enriching property of biodegradable polymers when composted as waste can strengthen green economy and reduce the greenhouse gas (GHG) load in the environment (Baghi *et al.,* 2022; Priyadarshi and Rhim, 2020; Sharma *et al.,* 2018).

Chitosan, a cationic polysaccharide derived from chitin in seafood waste, possesses unique nitrogen-containing functional groups. Its amino and hydroxyl moieties confer valuable chemical, biological, and functional properties, including solubility, film-forming capability, viscosity enhancement, chelation capacity, and intrinsic antimicrobial activity (Priyadarshi and Rhim, 2020; Sharma and Bhende, 2024). These attributes enable diverse applications in food, pharmaceuticals, biomedicine, and environmental technology (Sharma and Bhende, 2024). However, CH films often exhibit limitations in mechanical strength and barrier performance against water vapor. Blending with other polymers (Hiremani *et al.,* 2022) or incorporating active compounds (e.g. antioxidants (Souza *et al.,* 2017), polyphenols (Sun *et al.,* 2017), curcumin (Roy and Rhim, 2020), and syringic acid (Yang *et al.,* 2019) are common strategies to mitigate these weaknesses.

Guar gum, a galactomannan polysaccharide extracted from guar bean endosperms, is characterized by its high molecular weight, long polymer chains, and ability to form viscous aqueous solutions through extensive hydrogen bonding (Bhat *et al.,* 2022; Sharma *et al.,* 2018; Wang *et al.,* 2023). Its thickening, stabilizing, and emulsifying properties make it valuable in food, pharmaceutical, and industrial applications (Narasagoudr *et al.,* 2023; Sharma *et al.,* 2018). GG also demonstrates biocompatibility and strong film-forming potential (Gürdaş Mazlum *et al.,* 2025; Rao *et al.,* 2010; Wang *et al.,* 2023). However, GG-based films often have high aqueous solubility and poor mechanical properties. Combining GG with CH enhances performance; for instance, CH-GG composites (15% v/v GG) exhibit low oxygen permeability and improved tensile/puncture strength (Rao *et al.,* 2010). Cross-linked GG-CH films without plasticizers show enhanced water stability and mechanical integrity (Rahman *et al.,* 2021). Furthermore, incorporating GG into CH matrices reduces water solubility (WS), water vapor permeability (WVP), and flexibility while increasing opacity and tensile strength (TS) relative to pure CH films (Gürdaş Mazlum and Erdoğan, 2025).

Quince seed mucilage, obtained from the seeds of quince fruit, is a plant biopolymer, such as GG. When quince seeds are soaked in water, a mucilage containing soluble polysaccharides, amino acids, and cellulose is formed (Kozlu and Elmaci, 2020). QSM, a thickener with higher viscosity, thanks to its high molecular weight, is used as a stabilizer and gelling agent in the food industry. QSM, with its unique colloidal properties, low production cost, and easy extraction, is used as a polysaccharide source in edible film formulations (Emir Çoban *et al.,* 2024; Sarmadikia *et al.,* 2022). Using QSM produced from fruit waste as an edible film material is an environment-friendly and sustainable approach that promotes waste reduction.

In this respect, the preparation of edible films by adding QSM to CH and GG biopolymers constitutes the innovative aspect of the present study. QSM is a biopolymer that has been used in recent years as a basic component of edible films. In literature, few studies are found using QSM in edible films. For example, edible films were prepared by adding different concentrations of glycerol (Jouki *et al.,* 2013), thyme essential oil (Jouki *et al.,* 2014), and vitamin D3 (Behjati and Yazdanpanah, 2021), to QSM, and it was reported that the TS and surface hydrophobicity of the obtained films decreased and they showed antioxidant and antimicrobial activity. In studies where QSM was used as a component of coating solutions, mandarin slices (Kozlu and Elmaci, 2020), trout fillets (Sarmadikia *et al.,* 2022), and fresh walnut kernels (Yousuf and Maktedar, 2022) were coated with a coating solution. Once coated, the coating is found to be effective in preserving the quality of these foods and preventing spoilage. The amount of water present in films provides information about their hydrophilicity; more hydrophilic films offer the highest moisture content (MC) values (Hiremani *et al.,* 2022). QSM is a hydrophilic polymer, and this property limits its application as a standalone packaging film. When the MC of CH, GG and QSM films was examined, it was reported that the QSM film had the highest MC. In the same study, it was determined that the MC values of CH/QSM composite films decreased by 2.87%, compared to the CH control film (Gürdaş Mazlum *et al.,* 2025).

Chitosan, GG, and QSM are important biopolymers and have the potential to be alternatives to traditional plastic packaging materials. These three biopolymers are biocompatible, edible, sustainable, biodegradable, nontoxic, and capable of forming films, thus making them ideal components for edible films. The brittle and fragile structures of natural biopolymers, such as CH, GG, and QSM cause difficulties in film preparation. These polymers require plasticizers to reduce the frictional forces between polymer chains, such as hydrogen bonds or ionic forces, to improve their mechanical properties (Hiremani *et al.*, 2021). Therefore, in the present study, we chose glycerol as a plasticizer. Numerous studies are conducted using polymers such as CH, GG, and QSM by blending two of these polymers or by incorporating fillers, cross-linking agents, nanomaterials, and various active and functional compounds into each polymer (Behjati and Yazdanpanah, 2021; Emir Çoban *et al.,* 2024; Jouki *et al.,* 2014; Rahman *et al.,* 2021). However, the physicochemical, mechanical, and thermal properties of edible films have not yet been improved to the desired level. The use of CH, GG, and QSM polymers together for producing edible films can contribute to improving film properties. Apart from our studies, to our knowledge, no study has been conducted on the use of these three polymers together for producing edible films. In the first section of the study, the properties of the CH/GG/QSM-1 (5% GG/QSM) and CH/GG/QSM-2 (10% GG/QSM-1) composite films produced by adding GG/QSM to the CH film matrix were examined. It has been reported that the addition of GG/QSM to the CH film matrix increases the opacity of the composite films and improves their physicochemical and mechanical properties (Gürdaş Mazlum *et al.,* 2025). No comprehensive study has been conducted on the development of composite films containing 20%, 30% and 40% GG/QSM added to the CH film matrix and the detailed examination of their properties. Changes in the structure of composite films by increasing the addition of GG/QSM have not been reported yet. In this context, the second part of the study aims to examine comprehensively the physicochemical, barrier, optical, mechanical, thermal, and microstructural properties of CH-based composite films prepared by adding GG/QSM in different proportions (20%, 30%, and 40%) and to demonstrate their usability. The aim of using these biopolymers together is to investigate the possibility of producing composite films by developing their advantageous properties and minimizing their disadvantages through resulting interactions between film components.

Materials and Methods

Materials and chemicals

In Sivas, Turkey, quince fruits (*Cydonia oblonga*) were purchased from a neighborhood market. After removing the seeds manually, the same were cleaned thoroughly with distilled water and allowed to air dry at room temperature. GG, glycerol (plasticizer, ≥99.5%), CH (medium molecular weight: 1.9–3.1 × 10^5 Da, degree of deacetylation ≥75%, viscosity: 200–800 cP in 1% acetic acid), and all other chemicals were of analytical grade and purchased from Sigma-Aldrich (Steinheim, Germany). The experiments were conducted using deionized water.

Extraction of QSM

Quince seed mucilage was extracted by following established methods with minor modifications (Gürdaş Mazlum *et al.,* 2025; Jouki *et al.,* 2013). Briefly, 10 g of dried quince seeds were dispersed in 100 mL of distilled water (water–seed ratio was 100:10). The mixture was heated to 45°C in a water bath and stirred continuously for 15 min. Then the swollen seeds were blended, and the resulting mucilage was separated. The mucilage solution was filtered

through cheesecloth to remove coarse particles, and homogenized (Isolab homogenizer) at 12,000 rpm for 3 min. To eliminate air bubbles and insoluble matter, the homogenate was centrifuged at 4,000 rpm for 12 min. Supernatant (QSM extract) was collected, dried in a convection oven at 30°C, pulverized into a fine powder using a mortar and pestle, and at stored at 4°C. The method yielded approximately 15% extract based on dry weight of seeds.

Preparation of film-forming solutions and casting

Edible films were prepared by the casting method. In this study, composite films were prepared by mixing 1% (w/v) solution concentrations of CH, GG, and QSM. The main reasons for preferring 1% (w/v) concentration in the study were the solution viscosity being suitable for film casting, polymers dissolving completely, a homogeneous dispersion being achieved, the resulting films providing the desired thickness and transparency, and a reasonable balance achieved in mechanical/barrier properties. In addition, since hydrocolloids, such as GG and QSM, give high viscosity even at low concentrations, 1% level is generally reported as ideal in studies (Jouki *et al.,* 2013; Kozlu and Elmacı, 2020). In preliminary experiments, different proportions of GG and QSM were added to CH. However, the best homogeneity, casting, and drying properties were achieved with equal volumes of GG/QSM (1:1) added to CH. Therefore, variation with equal volumes of GG/QSM (1:1) was preferred when preparing CH-based composite films.

QSM solution (1%, w/v): In all, 1 g of QSM was dissolved by stirring in distilled water. 35% (w/w) glycerol based on QSM weight was added to the solution with constant stirring (750 rpm) at 45°C for 15 min (Jouki *et al.,* 2013). The solution was then homogenized at room temperature (750 rpm) and centrifuged (4,000 rpm, 12 min) to remove air bubbles.

Chitosan solution (1%, w/v*)*: In all, 1 g of CH was prepared by dissolving in 1% (v/v) acetic acid aqueous solution with stirring at 25°C for 4 h; 63% (w/w) glycerol, as plasticizer, was added into CH solution and stirred for additional 6 h (Gürdaş Mazlum *et al.,* 2025). The solution was centrifuged (4,000 rpm, 12 min) to remove air bubbles.

Guar gum solution (1%, w/v): In all, 1 g of GG was dissolved by stirring in distilled water. Then, 35% (w/w) glycerol was added to the solution, and it was made up to a final volume of 100 mL. The mixture was homogenized using a magnetic stirrer (750 rpm) until fully dissolved, followed by centrifugation (4,000 rpm, 12 min) to remove air bubbles (Gürdaş Mazlum and Erdoğan, 2025).

Composite film solutions: Preliminary experiments were conducted to optimize the ratio of GG and QSM to be added to CH. GG and QSM were added in a ratio of 1:1, and a more homogeneous mixture was obtained at this ratio.

Edible films were produced using the solution casting method. Composite film solutions were prepared by mixing 1% (w/v) CH, GG, and QSM stock solutions in the proportions specified in Table 1. The blend solutions were then homogenized at room temperature (750 rpm) and centrifuged (4,000 rpm, 12 min) to remove air bubbles. While preparing composite films, GG and QSM solutions of the same concentration were added in equal volumes (1:1). Concentration of GG and QSM (v/v) in the film formation mixture was determined as 0% (film A), 20% (film B), 30% (film C), and 40% (film D). Film solution, 10 mL, was poured on each 8-cm diameter Teflon plate and dried at 30°C for 24 h. Prior to conditioning, the dried films were carefully removed from casting surfaces and stored in a desiccator at room temperature, protected from light (Gürdaş Mazlum *et al.,* 2025). Films were equilibrated in a controlled humidity environment prior to characterization:

For physical, barrier, and mechanical property testing, the films were conditioned in a desiccator filled with a saturated solution of magnesium nitrate hexahydrate [$Mg(NO_3)_2 \cdot 6H_2O$] for 7 days to maintain 52% relative humidity (RH) at room temperature (about 25°C) to achieve moisture equilibrium.

Table 1. Compositions of CH, CH/GG/QSM1, CH/GG/QSM2, and CH/GG/QSM3 films.

Film		Chitosan (CH) (g/100 mL)	Guar Gum (GG) (g/100 mL)	Quince seeds mucilage (QSM) (g/100 mL)
CH	A	1	0	0
CH/GG/QSM1	B	0.80	0.1	0.1
CH/GG/QSM2	C	0.70	0.15	0.15
CH/GG/QSM3	D	0.6	0.20	0.20

The films were conditioned for 7 days at room temperature in a desiccator with silica gel (0% RH) for thermal analysis (differential scanning calorimetry [DSC]) and Fourier-transform infrared (FTIR) spectroscopy as well as to guarantee a dry state.

Physicochemical, barrier, optical, and mechanical properties of composite films

Thickness measurement

A digital micrometre was used to measure the thickness of the film at 10 different locations selected randomly (Dasqua, Italy; precision: 0.001 mm). Samples exhibiting defects (air bubbles, nicks, and tears) or thickness variations >5% were discarded. The mean thickness value was utilized in subsequent calculations of water vapor permeability (WVP) and mechanical properties (Kurt and Kahyaoğlu, 2014). Experiments were performed in triplicate, and the results were averaged.

Moisture content

The MC of edible films was determined using the drying oven method. A film sample measuring 1 × 3 cm was weighed and dried in a hot air oven at 105°C for 6 h. The MC was calculated as a percentage of the initial weight lost during the drying process (Roy and Rhim, 2020). Experiments were performed in triplicate, and the results were averaged.

Water solubility

The film was cut into 2 × 2 cm to determine solubility. The films were dried at 105°C for 24 h to determine initial dry mass (W_1). The film samples were placed in a beaker containing 30 mL of distilled water, covered with a parafilm, and stored at 25°C for 24 h (without shaking). After incubation, the samples were removed, dried in an oven at 105°C for 24 h, and weighed (W_2). WS was calculated using Equation (1) (Yang *et al.,* 2019). Experiments were performed in triplicate, and the results were averaged,

$$WS(\%) = \frac{(W_1 - W_2)}{W_1} \times 100, \quad (1)$$

where WS is water solubility of the sample (%); W_1 is the initial sample weight (g) and W_2 is the dry sample weight (g).

Water vapor permeability

The WVP of film samples was determined gravimetrically using a modified ASTM E96 method (Kurt and Kahyaoğlu, 2014). First, 1 g of silica gel was placed into 10-cm glass test tubes, and tube openings were sealed with film samples, which were secured using a parafilm. The tubes were then placed in a desiccator containing saturated magnesium nitrate hexahydrate to maintain an RH of 52% at 25°C. Weight gain was recorded daily over a period of 7 days, and a weight-versus-time graph was plotted. The WVP of films was calculated using Equation (2), based on the slope of the linear portion of weight–time curve. In Equation (2), w/t is the change in weight over time (g/s), determined by linear regression ($R^2 \geq 0.99$),

$$WVP = \frac{w}{t} \times \frac{x}{\Delta P \times A}, \quad (2)$$

where m is the mass increase (g), t is the time of permeation (s), x is the average film thickness (m), A denotes the exposed film surface area (m^2); and ΔP is the partial pressure difference (Pa). Equation (3) was used to calculate ΔP value in the WVP ($g \bullet s^{-1} \bullet m^{-1} \bullet Pa^{-1}$) equation.

$$\Delta P = S \times (R1 - R2). \quad (3)$$

In Equation (3), S represents the saturated vapor pressure of water at 25°C (3,168 Pa), $R1$ denotes RH of the desiccator environment, and $R2$ represents RH inside the tube (0% RH) (Kurt and Kahyaoğlu, 2014). Experiments were performed in triplicate, and the results were averaged.

Color properties

Color of the films was measured using a chroma meter (CR-400; Konica Minolta, Japan) color measurement device, which provided numerical values corresponding to three different color scales; L* (black to white, luminosity), a* (+red to –green), and b* (+yellow to -blue). The device, equipped using a D65 illuminant, an 8.0-mm aperture size, and a 10° standard observer angle, was calibrated using a white standard plate. Before measurements, samples were allowed to stabilize at room temperature for 10 min (blooming). Three readings were taken from different areas and recorded, and total color difference (ΔE) was calculated using equation (4). The measurement was done in triplicate, and the results were averaged.

$$\Delta E = \sqrt{(L^* - L)^2 + (a^* - a)^2 + (b^* - b)^2} \quad (4)$$

where L^*, a^*, and b^* are color parameter values of white standard backgrounds (L^* = 93.49, a^* = 0.25, and b^* = 0.09), and L, a, and b are color parameter values of a sample (Jouki *et al.,* 2013).

Opacity

Opacity was quantified via ultraviolet–visible spectra (UV-Vis) spectrophotometry (Optima SP 3000 Plus, Japan) at 600 nm (Souza *et al.,* 2017). The film sample strips were cut into rectangular sizes (3 × 1 cm) and placed in a cuvette and an empty cuvette was used as a reference. Measurements were performed using air as the reference. Absorbance values were recorded at 600 nm. Three measurements were made, and the average absorbance was determined. Film opacity was ascertained using the technique outlined by Souza *et al.* (2017). The measurement was done in triplicate and the average of three spectra was calculated. Opacity values were calculated using the absorbance data in Equation (5),

$$Opacity\ (mm^{-1}) = \frac{Abs_{600}}{\times}, \quad (5)$$

where x is the thickness (mm) and Abs_{600} is the absorbance value at a wavelength of 600 nm.

Mechanical properties

Tensile strength and elongation at break (EB) were measured using a 5-kg load cell at 24 ± 1°C and a texture analyser (TA.XTPlus, Stable Micro Systems, UK). Rectangular strips (60 × 10 mm) were mounted between grips (initial distance: 50 mm) and extended at 10 mm/s until rupture. The maximum force at break and EB were recorded using the software connected to the device. Tensile strength (MPa) and EB (%) were derived from stress–strain curves (Kurt and Kahyaoğlu, 2014). Experiments were performed in triplicate, and the results were averaged.

Structural characterization of films

The thermal characteristics of the samples were determined using DSC (Shimadzu DSC 60, Shimadzu Corporation, Japan). A 7-mg film sample, cut into small pieces, was analyzed at a heating rate of 10°C/min from 0°C to 400°C under a nitrogen atmosphere. The reference was an empty aluminum pan. The tests were conducted in duplicate and the results were averaged.

The chemical structure and functional groups of the films were investigated using FTIR (Mode Tensor 27; Bruker, USA). The analysis was carried out at a resolution of 4 cm^{-1} and in the range of 400–4,000 cm^{-1}.

Surfaces of the prepared composite edible films were coated with gold using a Quorum Q150R ES sputter coater. Morphological properties as well as the shape and size of the films were examined using scanning electron microscopy (SEM) (TESCAN MIRA3 XMU Brno, Czech Republic).

Statistical analysis

All experiments were performed in triplicate (n = 3). Statistical analysis was conducted using analysis of variance (ANOVA) with the Minitab Statistical Software Version 13 (Minitab Inc., State College, PA, USA). The results were expressed as mean ± standard error (SE). Tukey's multiple comparison test was applied to determine significant differences between mean values at a confidence level of $P < 0.05$. The correlation of parameters was evaluated by Pearson's correlation (Microsoft Office Excel 2016, Microsoft Corporation, USA).

Results and Discussion

Thickness and moisture content and water solubility of edible composite films

Film thickness is a critical parameter influencing WVP, mechanical strength, and optical characteristics. As presented in Table 2, the CH control film exhibited a thickness of 0.097 ± 0.009 mm. Composite films with thickness values ranging from 0.102 to 0.108 mm were produced by incorporating GG and QSM blends at 20–40% (v/v). According to statistical analysis, composite films (CH/GG/QSM1–3) and the control did not differ significantly ($P > 0.05$), suggesting that the addition of GG/QSM did not significantly change the dimensionality of films. This aligned with previous observations that addition of nanofillers may not significantly impact bionanocomposite film thickness (Emir Çoban *et al.*, 2024).

Moisture content varied substantially across formulations (Table 2). The CH control film displayed an MC of 29.787 ± 0.004%, while composites exhibited values spanning from 21.275 ± 0.006% to 37.791 ± 0.022%. The addition of 20% GG/QSM to CH film matrix resulted in the CH/GG/QSM1 composite film achieving the highest MC (37.791%; $P < 0.05$). This phenomenon was attributed to an increase in the number of water molecules present between polymer chains through hydrogen bonding. It was observed that the bond interactions and bond formations between CH, GG and QSM polymers caused shifts in the peak positions of FTIR spectrum (Figure 4). Similar results were reported by Jouki *et al.* (2014) for QSM films containing thyme essential oil. Conversely, increasing GG and QSM concentrations to 30% and 40%, respectively, significantly reduced MC ($P < 0.05$), with CH/GG/QSM3 exhibiting the lowest value (21.275%).

Table 2. Thickness, MC, WS, and WVP of CH, CH/GG/QSM1, CH/GG/QSM2, and CH/GG/QSM3 films.

Film type	Thickness (mm)	MC (%)	WS (%)	WVP × 10^{-11} ($g.s^{-1}.m^{-1}.Pa^{-1}$)
CH	0.097 ± 0.009^{b}	29.787 ± 0.004^{b}	20.12 ± 0.632^{a}	8.437 ± 0.004^{a}
CH/GG/QSM1	$0.102 \pm 0.004^{a,b}$	37.791 ± 0.022^{a}	16.379 ± 0.102^{b}	6.335 ± 0.038^{b}
CH/GG/QSM2	$0.107 \pm 0.009^{a,b}$	$28.155 \pm 0.003^{b,c}$	$19.626 \pm 0.014^{a,b}$	8.444 ± 0.002^{a}
CH/GG/QSM3	0.108 ± 0.024^{a}	21.275 ± 0.006^{c}	22.634 ± 1.427^{a}	8.444 ± 0.002^{a}

Notes: The values are presented as mean ± SE.
Values within each column with different superscripted alphabets are significantly different (P < 0.05).

This reduction suggests molecular interactions between GG, QSM, and CH limited water accessibility to CH's hydrophilic groups (Yang *et al.,* 2019), a phenomenon corroborated by FTIR evidence of amino-hydroxyl group interactions.

Water solubility, a key indicator of film integrity in aqueous environments and biodegradability (Hiremani *et al.*, 2021) also demonstrated concentration-dependent effects. The CH control film had a WS of 20.12 ± 0.632%. The CH/GG/QSM1 composite (20% GG/QSM) exhibited the lowest WS (16.379 ± 0.102%; $P<0.05$), indicating improved water resistance because of reduced hydrophilicity and molecular interactions between GG/QSM and CH hydroxyl groups (Jouki *et al.*, 2014). However, higher GG–QSM ratios (30–40%) increased WS significantly ($P < 0.05$), with CH/GG/QSM3 reaching 22.634 ± 1.427%. Increase in the WS of composite film was due to the hydrophilic groups of QSM and GG easily interacting with water molecules, increasing the hydrophilicity of composite film. Yang *et al.* (2019) also reported similar results.

Water vapor permeability

Water vapor permeability critically determines a film's utility in food preservation by modulating moisture transfer. Films with low WVP reduce moisture transfer from the external environment to food, thereby preventing or delaying food spoilage. A low WVP value is desirable for keeping food fresh (Sun *et al.*, 2017; Yang *et al.*, 2019). The CH control film displayed a WVP of $8.437 \pm 0.004 \times 10^{-11}$ $g{\cdot}s^{-1}{\cdot}m^{-1}{\cdot}Pa^{-1}$ (Table 2). Notably, the CH/GG/QSM1 composite (20% GG/QSM) achieved a 24.75% reduction in WVP ($6.335 \pm 0.038 \times 10^{-11}$ $g{\cdot}s^{-1}{\cdot}m^{-1}{\cdot}Pa^{-1}$; $P < 0.05$). Hydrogen bond interactions between CH/GG/QSM1 composite film, CH, and GG/QSM network led to a decrease in water affinity by reducing the availability of hydrophilic groups. As a result, the CH/GG/QSM1 composite film showed the lowest WVP (Riaz *et al.*, 2020). Dense and non-porous structure in SEM images supported this finding (Figure 5B). This trend of reduction in the WVP of CH/GG/QSM1 composite film was similar to the reports of Jouki *et al.* (2014) and Riaz *et al.* (2020). No significant difference was found in the WVP values of CH control film and the CH-based CH/GG/QSM2 and CH/GG/QSM3 composite films ($P > 0.05$). The formation of cross-linking network between CH and GG in composite films compresses the water vapor diffusion area by reducing the binding sites of water molecules, thus limiting the water vapor escape (Foghara *et al.,* 2020). The WVP values of composite films, ranging between 10^{-11} $g{\bullet}s^{-1}{\bullet}m^{-1}{\bullet}Pa^{-1}$, may reduce the respiration rate and moisture migration of fruits and vegetables, thereby preventing excessive water vapor transmission. These findings indicate that CH-based composite films containing GG/QSM can be used as packaging films.

Color and optical properties of edible composite films

The optical characteristics of packaging films, particularly color and opacity, significantly influence consumer acceptance. As shown in Table 3, incorporation of GG/QSM blends into CH matrices systematically altered color parameters. While lightness (L) values showed no significant difference ($P > 0.05$) between the CH control film and the 20% GG/QSM composite (CH/GG/QSM1), higher GG/QSM concentrations (30–40%) in CH/GG/QSM2 and CH/GG/QSM3 composites induced statistically significant reductions in L values ($P < 0.05$). These results demonstrate a concentration-dependent decrease in film brightness with increasing GG/QSM content, suggesting that the biopolymer additives impart progressive darkening effects.

The "a" values of CH and CH-based composite films incorporating GG/QSM1 and GG/QSM2 were found to differ significantly ($P < 0.05$). The positive "a" values

Table 3. Color values, including L, "a", "b," and ΔE, of CH, CH/GG/QSM1, CH/GG/QSM2, and CH/GG/QSM3 films.

Film type	L	a	b	ΔE
CH	89.66 ± 0.05[a]	0.78 ± 0.006[a]	-3.61 ± 0.035[d]	5.355 ± 0.014[a,b]
CH/GG/QSM1	89.49 ± 0.35[a]	0.50 ± 0.034[b]	-2.50 ± 0.22[c]	4.771 ± 0.416[b]
CH/GG/QSM2	87.76 ± 0.04[b]	0.22 ± 0.063[c]	-0.26 ± 0.00[a]	5.741 ± 0.040[a]
CH/GG/QSM3	87.79 ± 0.05[b]	0.23 ± 0.017[c]	-1.17 ± 0.04[b]	5.838 ± 0.042[a]

Notes: The values are presented as mean ± SE.
Values within each column with different superscripted alphabets are significantly different (P < 0.05).

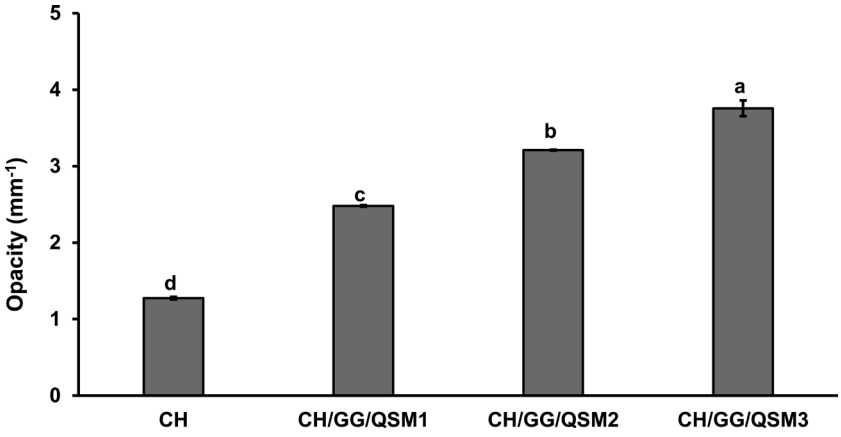

Figure 1. Opacity of CH, CH/GG/QSM1, CH/GG/QSM2, and CH/GG/QSM3 films. (Different letters indicate significant differences, *P* < 0.05).

of CH/GG/QSM1 and CH/GG/QSM2 films indicate a tendency toward red coloration, while values closer to zero suggest weaker color tones. The "b" value of the CH control film was measured as –3.61 ± 0.035. In composite films containing GG/QSM, the "b" values ranged from –2.50 ± 0.022 to –0.260 ± 0.00 ($P < 0.05$). Negative "b" values reflect a blue hue, and as these values approach zero with increased incorporation of GG/QSM, they indicate dilution in color intensity (Rahman *et al.*, 2021).

The total color difference (ΔE) of the CH control film was calculated to be 5.355 ± 0.014. The inclusion of GG/QSM into CH matrix had a limited impact on the ΔE values of composite films ($P < 0.05$). Similar ΔE results were reported by Rao *et al.* (2010) for CH-GG films containing 40% GG.

Compared to the control CH film, the opacity of CH-based composite films was noticeably higher. The opacity value of the control film was 1.273 ± 0.016 mm^{-1} (Figure 1), and there were statistically significant differences between the films ($P < 0.05$). The CH/GG/QSM1 film, formulated with 20% GG/QSM, exhibited an opacity value approximately double to that of the control ($P < 0.05$). This increase was attributed to structural compaction of film matrix, reducing the space between polymer chains, and thereby limiting light transmission (Wang *et al.*, 2021).

A consistent increase in opacity was observed with greater GG/QSM incorporation (Figure 1). Comparable trends were reported in CH films modified with syringic acid (SA) (Yang *et al.*, 2019). The CH/GG/QSM3 film, produced with 40% GG/QSM, showed an opacity value approximately three times higher than that of the control ($P < 0.05$). Rao *et al.* (2010) produced CS/GG composite films by adding GG at 20–40% (v/v) concentration to CH solution and reported that opacity decreased with increasing GG concentration. In the present study, increase in opacity with increasing GG/QSM ratio is attributed to QSM polymer. Among the prepared CH, GG, and QSM films, the highest opacity value was reported for QSM film (Gürdaş Mazlum *et al.*, 2025). Given the inverse relationship between opacity and transparency, increased opacity implies decreased transparency. This property could be beneficial for food packaging, as higher opacity helps to shield products from ultraviolet (UV) radiation (Jiang *et al.*, 2022).

Mechanical properties of edible composite films

Mechanical properties of edible films serve as vital markers of their robustness and durability, because they show how well they can preserve structural integrity and safeguard food items during handling and storage. For edible films to perform effectively in packaging applications, they must possess adequate mechanical strength and flexibility to resist external stress (Souza *et al.*, 2017; Wang *et al.*, 2021). Two key parameters used to evaluate these properties are TS and EB, which, respectively, indicate a film's ability to stretch without failure and its resistance to break. Both TS and EB values of the tested films are presented in Figure 2.

The CH control film's TS was 11.45 ± 1.075 MPa. The TS of the CH-based composite films made with different GG–QSM ratios varied. Among these, the CH/GG/QSM1 composite film exhibited the lowest TS, while the CH/GG/QSM2 film showed the highest TS value ($P < 0.05$). These mechanical trends were consistent with the physicochemical data. Specifically, CH/GG/QSM1 film, which included 20% GG/QSM, exhibited increased MC (Table 2), contributing to enhanced flexibility but reduced TS (Figure 2) (Foghara *et al.*, 2020).

When the GG/QSM concentration was increased from 30% to 40%, TS decreased from 13.12 ± 1.50 MPa to 9.97 ± 0.81 MPa. A similar pattern was observed by Yang *et al.* (2019) in CH films containing syringic acid. These findings suggest that the mechanical behavior of CH-based films is influenced by their polymeric matrix structure. At optimal concentrations, GG/QSM can enhance film strength by promoting intermolecular interactions and network formation. However, higher concentrations may disrupt the ordered polymeric matrix structure by weakening hydrogen bonding and reducing cohesive interactions between polymers. This disruption creates more flexible regions within the film, ultimately compromising mechanical strength (Sun *et al.*, 2017; Yang *et al.*, 2019).

Elongation at break reflects a film's ductility, that is, its capacity to stretch under stress before breaking. Typically, films with high EB values exhibit lower TS, indicating an inverse relationship between flexibility and strength (Bhat *et al.*, 2022). EB of the CH control

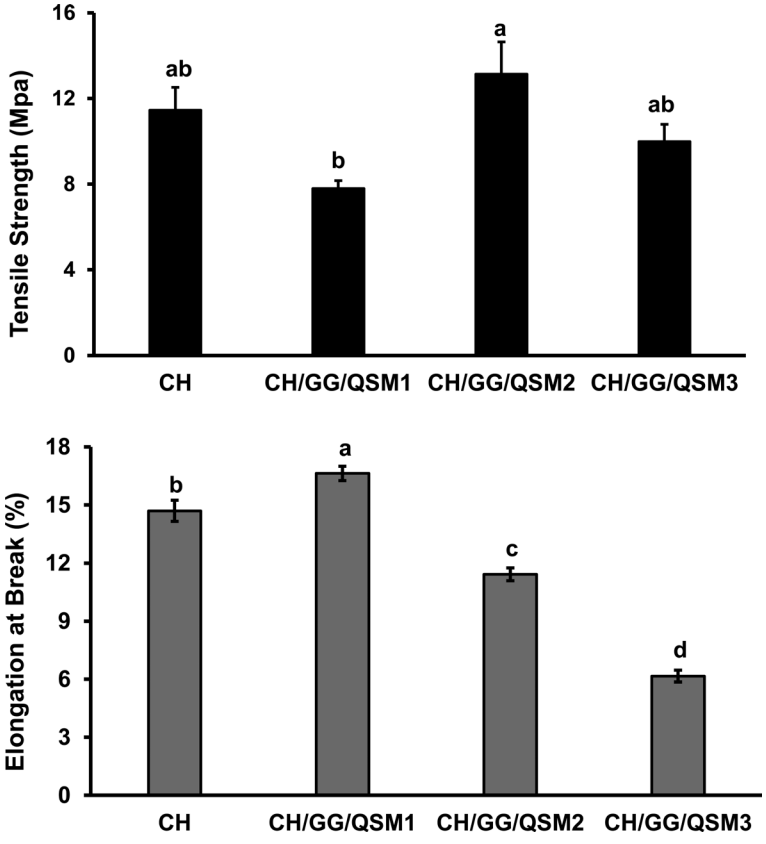

Figure 2. Tensile strength (TS) and elongation at break (EB) of CH, CH/GG/QSM1, CH/GG/QSM2, and CH/GG/QSM3 films (different letters indicate significant differences, $P < 0.05$).

film was 14.7 ± 0.54%. In composite films, EB values ranged from 6.16 ± 0.02% to 16.64 ± 0.369%, with GG/QSM addition having a statistically significant effect on this variability ($P < 0.05$). The CH/GG/QSM1 film demonstrated an increased EB compared to the control ($P < 0.05$), potentially because of the plasticizing effect of moisture. However, further increase in GG/QSM (CH/GG/QSM2 and CH/GG/QSM3) resulted in a significant decline in EB values ($P < 0.05$). This decrease suggests that stronger intermolecular interactions between CH, GG, and QSM reduce polymer chain mobility, thereby diminishing flexibility (Tang *et al.*, 2018). Overall, the CH/GG/QSM2 formulation, containing 30% GG/QSM, demonstrated the most balanced mechanical performance, combining both strength and moderate flexibility, making it a promising candidate for edible film applications.

Correlation analysis

Pearson's correlation analysis analyzes whether there is a significant relationship between two variables. The Pearson's correlation coefficient is used to examine strength and direction of the linear relationship between two continuous variables, and the letter "r" denotes correlation coefficient. Relationship (or correlation) between two variables is expressed as a number ranging from –1 to +1 (Hanif *et al.*, 2025).

The correlation between thickness, MC, WS, WVP, TS, EB, and opacity of composite films was investigated by Pearson's correlation and is shown in Table 4. Pearson's correlation explains that WS values decrease with increase in MC. An inverse relationship between MC and WS is observed in Table 2. While a strong negative linear relationship is observed between WVP and MC, a strong positive correlation is determined between WVP and WS. The Pearson's correlation indicates that as WS increases, WVP also increases (Table 2). According to Pearson's correlation coefficient, TS showed a moderate negative correlation with MC, while it showed a moderate positive correlation with WS. On the other hand, a strong positive correlation between TS and WVP indicated that TS increased with increase in WVP (Table 2). EB showed a strong negative correlation with thickness and WS, while a very strong positive correlation was observed with MC. EB had a moderate negative correlation with WVP. Opacity showed a strong positive correlation with thickness, while it showed a strong negative correlation with EB. This showed that while opacity and thickness increased together, opacity decreased with increase in EB. A moderate negative correlation was observed between opacity and MC.

Thermal analysis

Differential scanning calorimetry was used to assess edible composite films' thermal characteristics. As shown in thermograms (Figure 3), all films—including pure CH and CH-based composites—exhibited a two-stage thermal degradation profile. The DSC curves revealed two endothermic peaks and one exothermic peak, consistent with the findings reported in the literature (Emir Çoban *et al.,* 2024; Hiremani *et al.,* 2022). Table 5 presents the estimated values of glass transition temperature (T_g) and thermal decomposition temperature (T_{td}) for both CH and composite films. The first endothermic peak, observed in all samples, corresponds to moisture loss, indicating the evaporation of bounded water from films (Hiremani *et al.,* 2022). T_g values, located near this initial endothermic event, were recorded as follows: 117°C for pure CH, 149°C for CH/GG/QSM1, 120°C for CH/GG/QSM2, and 107°C for CH/GG/QSM3. T_g marks transition from a glassy, rigid state to a rubbery and more flexible state and reflects changes in the amorphous regions of polymer matrix (Hiremani *et al.*, 2021). The second endothermic peak observed in all samples is attributed to the thermal degradation of glycerol, which was used as a plasticizer in film formulations (Emir Çoban *et al.*, 2024). The corresponding temperatures were recorded as 230°C for CH, 243°C for CH/GG/QSM1, 236°C for CH/GG/QSM2, and 231°C for CH/GG/QSM3.

Table 4. Pearson's correlation analysis of CH, CH/GG/QSM1, CH/GG/QSM2, and CH/GG/QSM3 films.

	Thickness (mm)	MC (%)	WS (%)	WVP × 10^{-11} ($g.s^{-1}.m^{-1}.Pa^{-1}$)	TS (MPa)	EB (%)
MC (%)	–0.543					
WS (%)	0.389	–0.984				
WVP × 10^{-11} ($g.s^{-1}.m^{-1}.Pa^{-1}$)	0.201	–0.840	0.859			
TS (MPa)	0.138	–0.463	0.439	0.823		
EB (%)	–0.758	0.946	–0.887	–0.683	–0.275	
Opacity (mm^{-1})	0.989	–0.532	0.386	0.127	0.006	–0.967

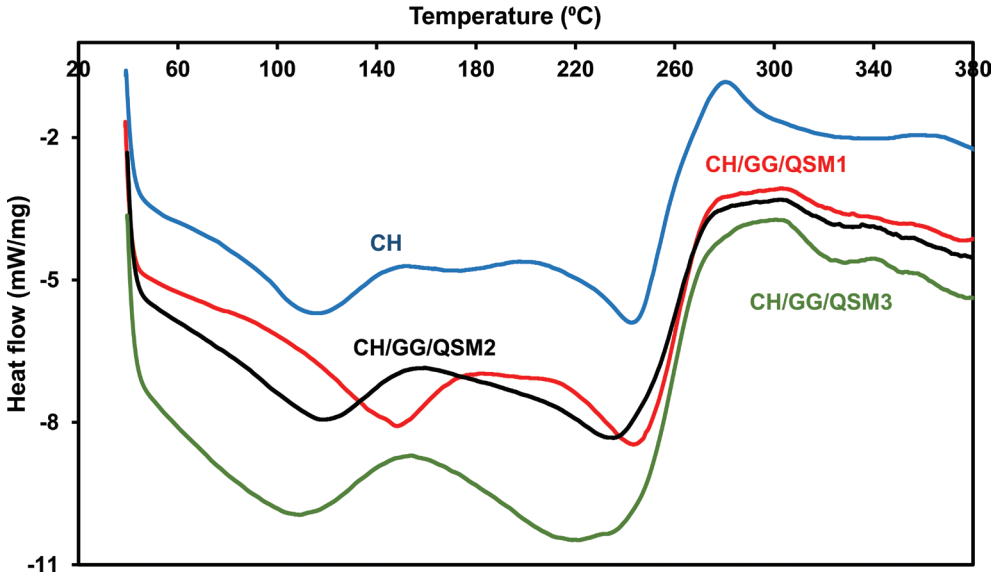

Figure 3. DSC thermograms of CH, CH/GG/QSM1, CH/GG/QSM2, and CH/GG/QSM3 films.

Table 5. Tg, and Ttd values of CH, CH/GG/QSM1, CH/GG/QSM2, and CH/GG/QSM3 films.

Film type	Tg (ºC)	Ttd (ºC)
CH	117 ± 1.0^{b}	282 ± 0.5^{b}
CH/GG/QSM1	149 ± 0.5^{a}	306 ± 1.0^{a}
CH/GG/QSM2	120 ± 0.5^{b}	307 ± 0.5^{a}
CH/GG/QSM3	107 ± 1.0^{c}	306 ± 0.5^{a}

Notes: The values are presented as mean ± SE.
Values within each column with different superscripted alphabets are significantly different (P < 0.05).

In pure CH film, an exothermic peak was observed at 279.36°C, corresponding to the thermal decomposition of polysaccharide backbone (Yang *et al.,* 2019). In contrast, the composite films exhibited exothermic peaks in the range of 306–307°C. The decomposition of CH, GG, and QSM components is linked to these higher T_{td} values, suggesting that composite films had better thermal stability than the control CH film. This improvement in thermal resistance is probably due to the formation of a more compact and cross-linked network within the polymer matrix on incorporation of GG/QSM. Similar enhancements in thermal behavior were observed by Hiremani *et al.* (2022) in CHOS composite films containing oxidized maize starch (OMS). Thermal stability is strongly influenced by crystallinity of the material, with higher crystallinity requiring more thermal energy for decomposition (Sun *et al.*, 2017). The elevated T_{td} values of composite films suggest that GG/QSM incorporation promotes a more ordered internal structure, thereby increasing thermal resistance.

Structural properties (FTIR analysis of films)

The FTIR spectra of CH and CH-based composite films are presented in Figure 4. In the spectrum of pure CH film, a broad absorption band centered at 3,268 cm^{-1}, corresponding to the stretching vibrations of O–H and N–H groups, which are indicative of strong hydrogen bonding (Hiremani *et al.,* 2022). Characteristic peaks at 2,920 cm^{-1} and 2,873 cm^{-1} are associated with symmetric and asymmetric C–H stretching vibrations, typical of polysaccharide structures (Emir Çoban *et al.*, 2024).

The C=O stretching vibration of amide I is attributed to the peak at 1,644 cm^{-1}, whereas the N–H bending vibration of amide II is associated with the band at 1,553 cm^{-1}. Additional peaks include a band at 1,407 cm^{-1} (O–H bending vibration), a sharp peak at 1,026 cm^{-1} (C–OH stretching) (Emir Çoban *et al.,* 2024; Hiremani *et al.,* 2022; Roy and Rhim, 2020), and bands at approximately 1,377 cm^{-1} (C–H bending vibrations). The peak observed at 1,320 cm^{-1} corresponds to the C=N stretching of amide III, while smaller peaks at 1,262 cm^{-1} and 1,204 cm^{-1} are attributed to the bending vibrations of hydroxyl groups and C–O stretching, respectively (Fernandes *et al.*, 2014; Menazea *et al.*, 2020). A prominent absorption at 1,152 cm^{-1} is associated with C–O stretching from β(1→4) glycosidic linkages, characteristic of CH's polysaccharide backbone. Additionally, a minor band at 926 cm^{-1} is attributed to C–H oscillatory vibrations from the saccharide structure (Menazea *et al.,* 2020). These spectral features are consistent with previous reports and confirm the presence of functional groups typical of

CH (Emir Çoban *et al.*, 2024; Hiremani *et al.*, 2022; Menazea *et al.*, 2020; Roy and Rhim, 2020).

When analyzing the spectra of composite films incorporating varying concentrations of GG/QSM into CH matrix, all major characteristic peaks of CH were retained, with the exception of C–O stretching band at 1,204 cm^{-1}, which was not observed clearly. Moreover, minor shifts were noted in several peak positions compared to pure CH spectrum. These spectral shifts suggest molecular interactions, potentially involving hydrogen bonding between the functional groups of CH and those of GG and QSM. Such interactions may contribute to changes in the physicochemical and structural properties of composite films.

The peak at 3,268 cm^{-1} in CH spectrum, attributed to hydrogen bonding interactions between amino and hydroxyl groups, shifted to 3,264 cm^{-1}, 3263 cm^{-1} and 3274 cm^{-1} in CH/GG/QSM1, CH/GG/QSM2, and CH/GG/QSM3 composite films, respectively, indicating strengthening of hydrogen bonds (Narasagoudr *et al.*, 2023). Similarly, peak at 2,920 cm^{-1}, corresponding to symmetric C–H stretching in CH, appeared at 2,924 cm^{-1}, 2,925 cm^{-1}, and 2,922 cm^{-1} in respective composite films. These spectral shifts suggest modifications in the chemical environment because of interactions between film components.

Further comparison of the spectra revealed slight shifts in characteristic bands ranging from 1,650 cm^{-1} to 648 cm^{-1} in composite films relative to pure components (CH, GG, and QSM), although no significant changes were observed in peak intensity. These subtle shifts are attributed to hydrogen bonding interactions between CH, GG, and QSM molecules. The displacement of absorption bands associated with hydroxyl, amino, and amide functional groups supports the miscibility of three biopolymers and suggests the formation of intermolecular hydrogen bonds and chemical interactions within composite matrix (Emir Çoban *et al.*, 2024; Wang *et al.*, 2023). These observations were consistent with the findings reported in previous studies, which highlight the ability of such biopolymer combinations to interact at molecular level, thereby influencing the physicochemical properties of the resulting films (Emir Çoban *et al.*, 2024; Wang *et al.*, 2023).

Microstructure of composite films

Scanning electron microscopy was employed to investigate the surface microstructures of CH and CH-based composite films, with representative images presented in Figure 5.

The CH control film appears to have a slightly rough and homogeneous surface (Figure 5A). Composite films produced by incorporating different ratios of GG/QSM into CH exhibited a smooth, homogeneous, nonporous, and dense surface (Figures 5B–D). Addition of GG/QSM significantly improved the

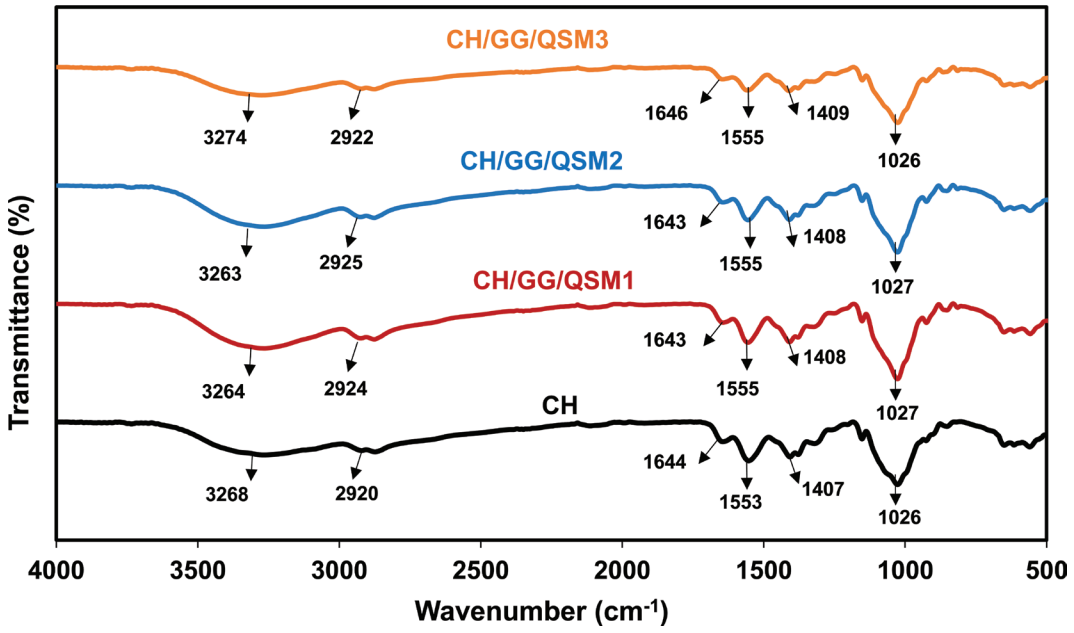

Figure 4. FTIR spectrums of CH, CH/GG/QSM1, CH/GG/QSM2, and CH/GG/QSM3 films.

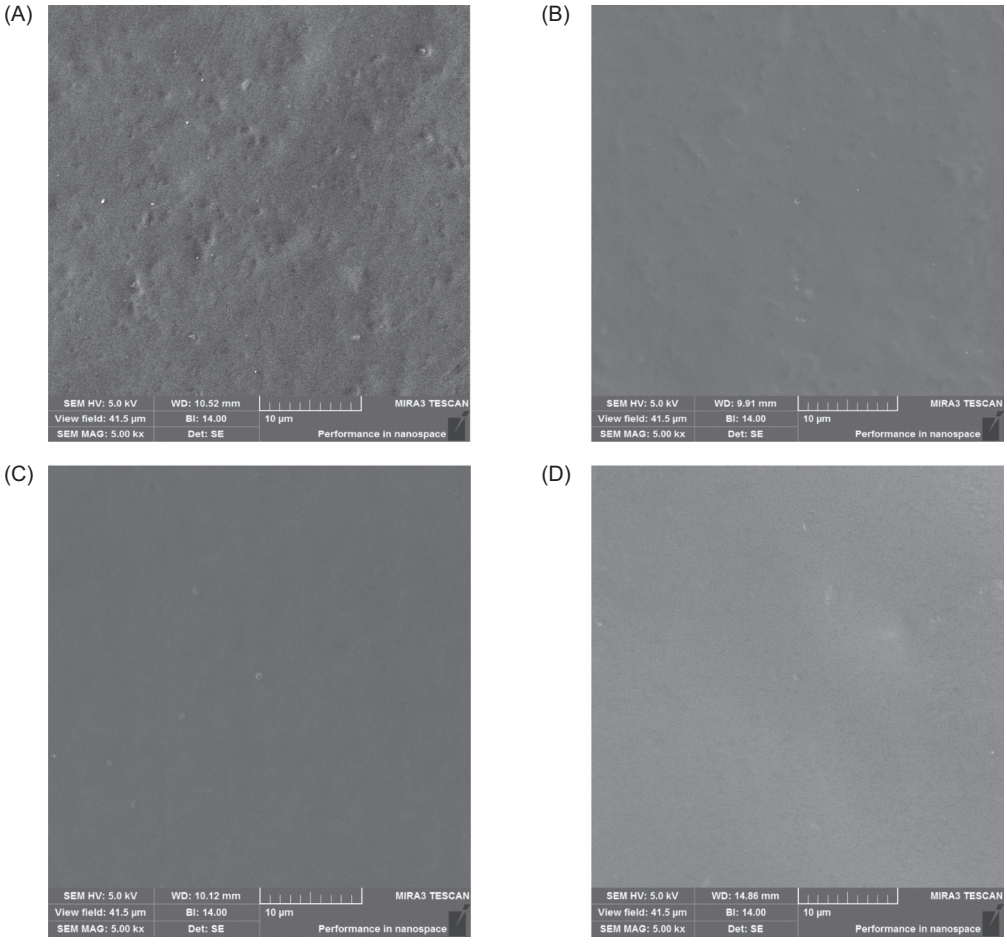

Figure 5. The SEM observation of films: (A) CH, (B) CH/GG/QSM1, (C) CH/GG/QSM2, and (D) CH/GG/QSM3. Magnification: 1,000×; Scale bar: 10 µm.

microstructures of composite films. Chitosan, QSM, and GG showed good compatibility and indicated that biopolymers were distributed evenly. Formation of hydrogen bonds between CH, QSM, and GG contributed to a uniform internal network structure (Wang *et al.,* 2023).

Limitations of the study and practical applications in the food industry

Although this study successfully demonstrated the development and characterization of CH-based composite films incorporating GG and QSM, several limitations should be acknowledged. First, the investigation focused primarily on the physical, mechanical, optical, and barrier properties of the films, while their antimicrobial and antioxidant activities were not evaluated. In addition, the long-term stability and biodegradability of the films under real food storage conditions were not examined, which limits the practical applicability of the findings. Moreover, the study was conducted under controlled laboratory conditions; therefore, the performance of these composite films when in direct contact with actual food matrices remains to be verified. Future research should address these limitations by exploring the films' active functional properties, storage behavior, and compatibility with various food products to better assess their potential for industrial applications.

Edible films are primary packagings that can be consumed along with food. Edible films are produced in thin sheets and then wrapped around the food surface or used in food packaging. (Cazón *et al.*, 2017). The prepared composite films show promising potential for practical applications in the food industry, particularly as a primary packaging for fresh fruits, vegetables, minimally processed foods, and moisture-sensitive products. Their improved barrier and mechanical properties could help

reduce moisture loss during storage. In addition, their natural and environment-friendly composition aligns with the growing demand for sustainable food packaging alternatives.

Conclusions

In this study, CH-based edible composite films were successfully developed using CH, QSM, and GG biopolymers. Results from DSC and SEM analyses demonstrated that the incorporation of GG/QSM polymers enhanced the thermal stability and microstructural uniformity of the films, compared to the pure CH control. FTIR analysis confirmed the existence of hydrogen bonding interactions among CH, GG, and QSM, which is evident from the differences in MC, WS and WVP values of composite films. All composite films exhibited higher opacity values than the control film. When compared to the CH control film, the CH/GG/QSM1 composite film exhibited the lowest WS and WVP values, while the CH/GG/QSM3 composite film exhibited the lowest MC values. The TS of CH/GG/QSM2 film increased by 14.58%, from 11.45 MPa to 13.12 MPa, while its EB decreased by 3.28%, from 14.70% to 11.42%. Among composite films, the CH/GG/QSM2 composite film demonstrated better mechanical properties. At the same time, while the MC, WS, and WVP values of the CH/GG/QSM2 composite film decreased compared to the pure CH film, it was determined that this composite film exhibited the best physicochemical properties. These improvements are attributed to the compatibility and synergistic interactions among CH, GG, and QSM, which contributed to enhanced opacity, MC, WS, WVP, thermal stability, and mechanical characteristics. When physicochemical, optical, mechanical, thermal, and microstructural properties of all composite films were compared, it was determined that the CH/GG/QSM2 film had the best properties.

The environment-friendly and sustainable properties of biopolymers of CH and QSM produced from food waste have great potential for the food packaging industry. CH, GG, and QSM are significant biopolymers for producing edible composite films as alternatives to traditional plastic food packaging because of their biodegradability, easy availability and nontoxic quality. Our findings indicate that biodegradable composite films are suitable for use as edible food packaging materials for fruits, vegetables, and food products because of their improved WVP and optical properties. It is anticipated that the composite films produced in this study would provide important information to literature and researchers working in this field. For a more complete characterization of these composite films, their antimicrobial and antioxidant properties must be evaluated. Nevertheless, further investigation is necessary to assess how these composite films interact with real food matrices to ascertain their practicality in actual food packaging situations.

Data Availability Statement

The data are available from the corresponding author upon request.

Ethical Approval

This research did not involve human or animal studies; therefore, no ethical approval was required.

Acknowledgments

This study constitutes a component of Aslı Eda Erdoğan's Master's thesis. The authors are indebted to the Scientific Research Projects Unit (CUBAP) of Sivas Cumhuriyet University for their financial support (M-668).

Author Contributions

Sevim Gürdaş Mazlum: project administration, supervision, conceptualization, funding acquisition, visualization, writing of original draft, and reviewing and editing. Aslı Eda Erdoğan: formal analysis, investigation, data curation, and visualization. Both writers gave their approval to the final manuscript.

Conflict of Interest

The authors declared no competing interests.

Funding

This research received no external funding.

References

Baghi, F., Gharsallaoui, A., Dumas, E. and Ghnimi, S. 2022. Advancements in biodegradable active films for food packaging: effects of nano/microcapsule incorporation. Foods 11(5):760. https://doi.org/10.3390/foods1105076

Behjati, J. and Yazdanpanah, S. 2021. Nanoemulsion and emulsion vitamin D3-fortified edible film based on quince seed gum. Carbohydrate Polymers 262:117948. https://doi.org/10.1016/j.carbpol.2021.117948

Bhat, V.G., Narasagoudr, S.S., Masti, S.P., Chougale, R.B., Vantamuri, A.B. and Kasai, D. 2022. Development and evaluation of Moringa extract incorporated chitosan/guar gum/polyvinyl alcohol active films for food packaging applications. International Journal of Biological Macromolecules 200:50–60. https://doi.org/10.1016/j.ijbiomac.2021.12.116

Cazón, P.G., Velazquez, J.A. and Ramírez, M. 2017. Vázquez, polysaccharide-based films and coatings for food packaging: a review. Food Hydrocolloids 68:136–148. https://doi.org/10.1016/j.foodhyd.2016.09.009

Emir Çoban, O., Akat, Z., Karatepe, P. and İncili, G.K. 2024. *In vitro* bioactivity of biodegradable films based on chitosan/quince seed mucilage reinforced with ZnO-nanoparticle. Food Measure 18:5450–5461. https://doi.org/10.1007/s11694-024-02579-7

Fernandes Q.M., Melo, K.R., Sabry, D.A., Sassaki, G.L. and Rocha, H.A. 2014. Does the use of chitosan contribute to oxalate kidney stone formation? Marine Drugs 13(1):141–158. https://doi.org/10.3390/md13010141

Foghara, S.K., Jafarian, S., Zomorodi, S., Asl, A.K. and Nasiraei, L.R. 2020. Fabrication and characterization of an active bionanocomposite film based on basil seed mucilage and ZnO nanoparticles. Journal of Food Measurement and Characterization 14:3542–3550. https://doi.org/10.1007/s11694-020-00588-w

Gürdaş Mazlum, S. and Erdoğan, A.E. 2025. Guar gum ilaveli kitosan kompozit filmlerin karakterizasyonu. Gıda 50(4):506–518. https://doi.org/10.15237/gida.GD25048

Gürdaş Mazlum, S., Erdoğan, A.E. and Kütük, N. 2025. Characterization of edible film produced from chitosan, quince seed mucilage and guar gum. Journal of Food Measurement and Characterization 19:8316–8332. https://doi.org/10.1007/s11694-025-03536-8

Hanif, M.F., Hashem, A.F., Hussain, HM., Siddiqui, M.K. 2025. A statistical correlation of entropy measures and zagreb indices in antizeolite networks via Pearson's analysis. Chemical Papers 79:6985–6997. https://doi.org/10.1007/s11696-025-04240-z

Hiremani, V.D., Gasti, T., Masti, S.P., Malabadi, R.B. and Chougale, R.B. 2022. Polysaccharide-based blend films as a promising material for food packaging applications: physicochemical properties. Iranian Polymer Journal 31:503–518. https://doi.org/10.1007/s13726-021-01014-8

Hiremani, V.D., Khanapure, S., Gasti, T., Goudar, N., Vootla, S.K., Malabadi, R.B., Mudigoudra, B.S. and Chougale, R.B. 2021. Preparation and physicochemical assessment of bioactive films based on chitosan and starchy powder of white turmeric rhizomes (*Curcuma zedoaria*) for green packaging applications. International Journal of Biological Macromolecules 193:2192–2201. https://doi.org/10.1016/j.ijbiomac.2021.11.050

Jiang, L., Wang, F., Xie, X., Xie, C., Li, A., Xia, N., Gong, X. and Zhang, H. 2022. Development and characterization of chitosan/guar gum active packaging containing walnut green husk extract and its application on fresh-cut apple preservation. International Journal of Biological Macromolecules 209:1307–1318. https://doi.org/10.1016/j.ijbiomac.2022.04.145

Jouki, M., Mortazavi, S.A., Yazdi, F.T. and Koocheki, A. 2014. Characterization of antioxidant-antibacterial quince seed mucilage films containing thyme essential oil. Carbohydrate Polymers 99:537–546. https://doi.org/10.1016/j.carbpol.2013.08.077

Jouki, M., Yazdi, F.T., Mortazavi, S.A. and Koocheki, A. 2013. Physical, barrier and antioxidant properties of a novel plasticized edible film from quince seed mucilage. International Journal of Biological Macromolecules 62:500–507. https://doi.org/10.1016/j.ijbiomac.2013.09.031

Kozlu, A. and Elmaci, Y. 2020. Quince seed mucilage as edible coating for mandarin fruit; determination of the quality characteristics during storage. Journal of Food Processing and Preservation 44(11), e14854. https://doi.org/10.1111/jfpp.14854

Kurt, A. and Kahyaoğlu, T. (2014). Characterization of a new biodegradable edible film made from salep glucomannan. Carbohydrate Polymers 104:50–58. https://doi.org/10.1016/j.carbpol.2014.01.003

Maurizzi, E., Bigi, F., Quartieri, A., De Leo, R., Volpelli, L.A. and Pulvirenti, A. 2021. The green era of food packaging: general considerations and new trends. Polymers 14(20):4257. https://doi.org/10.3390/polym14204257

Menazea, A.A., Ismail, A.M., Awwad, N.S. and Ibrahium, H.A. 2020. Physical characterization and antibacterial activity of PVA/chitosan matrix doped by selenium nanoparticles prepared via one-pot laser ablation route. Journal of Materials Research and Technology 9(5):9598–9606. https://doi.org/10.1016/j.jmrt.2020.06.077

Narasagoudr, S.S., Masti, S.P., Hegde, V.G. and Chougale, R.B. 2023. Cetrimide crosslinked chitosan/guar gum/gum ghatti active biobased films for food packaging applications. Journal of Polymers and the Environment 31:579–594. https://doi.org/10.1007/s10924-022-02655-3

Priyadarshi, R. and Rhim, J. 2020. Chitosan-based biodegradable functional films for food packaging applications. Innovative Food Science & Emerging Technologies 62:102346. https://doi.org/10.1016/j.ifset.2020.102346

Rahman, S., Konwar'a, A., Majumdar, G. and Chowdhury, D. 2021. Guar gum-chitosan composite film as excellent material for packaging application. Carbohydrate Polymer Technologies and Applications 2:100158. https://doi.org/10.1016/j.carpta.2021.100158

Rao, M.S., Kanatt, S.R., Chawla, S.P. and Sharma, A. 2010. Chitosan and guar gum composite films: preparation, physical, mechanical and antimicrobial properties. Carbohydrate Polymers 82(4):1243–1247. https://doi.org/10.1016/j.carbpol.2010.06.058

Riaz, A., Lagnika, C., Abdin, M., Hashim, M.M. and Ahmed, W. 2020. Preparation and characterization of chitosan/gelatin-based active food packaging films containing apple peel nanoparticles. Journal of Polymers and the Environment 28:411–420. https://doi.org/10.1007/s10924-019-01619-4

Roy, S.J. and Rhim, W. 2020. Preparation of carbohydrate-based functional composite films incorporated with curcumin. Food Hydrocolloids 98:105302. https://doi.org/10.1016/j.foodhyd.2019.105302

Sarmadikia, M., Mohammad, M., Khezerlou, A., Hamishehkar, H. and Ehsani, A. 2022. Effect of microencapsulated bitter orange peel extract in coatings based on quince seed mucilage on the quality of rainbow trout fillet. Journal of Food Measurement and Characterization 16(5):3877–3887. https://doi.org/10.1007/s11694-022-01442-x

Sharma, S. and Bhende, M. 2024. An overview: nontoxic and eco-friendly polysaccharides—its classification, properties, and diverse applications. Polymer Bulletin 81:12383–12429. https://doi.org/10.1007/s00289-024-05307-9

Sharma, G., Sharma, S., Kumar, A., Al-Muhtaseb, A.H., Naushad M., Ghfar, A.A., Mola, G.T. and Stadler, F.J. 2018. Guar gum and its composites as potential materials for diverse applications: a review. Carbohydrate Polymers 199:534–545. https://doi.org/10.1016/j.carbpol.2018.07.053

Souza, V.G.L., Fernando, A.L., Pires, J.R.A., Rodrigues, P.F., Lopes, A.A. and Fernandes, F.M.B. 2017. Physical properties of chitosan films incorporated with natural antioxidants. Industrial Crops and Products 107:565–572. https://doi.org/10.1016/j.indcrop.2017.04.056

Sun, L., Sun, J., Chen, L., Niu, P., Yang, X. and Guo, Y. 2017. Preparation and characterization of chitosan film incorporated with thinned young apple polyphenols as an active packaging material. Carbohydrate Polymers 163:81–91. https://doi.org/10.1016/j.carbpol.2017.01.016

Tang, Y., Zhang, X., Zhao, R., Guo, D. and Zhang, J. 2018. Preparation and properties of chitosan/guar gum/nanocrystalline cellulose nanocomposite films. Carbohydrate Polymers 197:128–136. https://doi.org/10.1016/j.carbpol.2018.05.073

Wang, H., Ding, F., Ma, L. and Zhang, Y. 2021. Edible films from chitosan-gelatin: physical properties and food packaging application. Food Bioscience 40:100871. https://doi.org/10.1016/j.fbio.2020.100871

Wang, F., Xie, C., YeR, Tang, H., Jiang, L and Liu, Y. 2023. Development of active packaging with chitosan, guar gum and watermelon rind extract: characterization, application and performance improvement mechanism. International Journal of Biological Macromolecules 227:711–725. https://doi.org/10.1016/j.ijbiomac.2022.12.210

Yang, K., Dang, H., Liu, L., Hu, X., Li, X., Ma, Z., Wang, X. and Ren, T. 2019. Effect of syringic acid incorporation on the physical, mechanical, structural and antibacterial properties of chitosan film for quail eggs preservation. International Journal of Biological Macromolecules 141:876–884. https://doi.org/10.1016/j.ijbiomac.2019.08.045

Yousuf, S. and Maktedar, S.S. 2022. Influence of quince seed mucilage-alginate composite hydrogel coatings on quality of fresh walnut kernels during refrigerated storage. Journal of Food Science and Technology – Mysore 59(12):4801–4811. https://doi.org/10.1007/s13197-022-05566-2